Impact of fine divertor geometrical features on the modelling of JET corner configurations

P. Tamain, H. Bufferand, G. Ciraolo, C. Giroud, Y Marandet, F. Militello, D.
Moulton, N. Vianello

Impact of fine divertor geometrical features on the modelling of JET corner configurations

P. Tamain[a], H. Bufferand[a], G. Ciraolo[a], C. Giroud[b], Y. Marandet[c], F. Militello[b], D. Moulton[b], N. Vianello[d], JET contributors

[a] CEA, IRFM, F-13108 Saint-Paul-lez-Durance, France
[b] UKAEA-CCFE, Culham Science Centre, Abingdon, Oxon, OX14 3DB, United Kingdom
[c] Aix-Marseille Univ, CNRS, PIIM, Marseille, France
[d] Consorzio RFX (CNR, ENEA, INFN, UNIPD, Acciaierie Venete SpA), Corso Stati Uniti 4 35127 Padova, Italy

Abstract

The modelling of JET corner configurations, in which the strike points are positioned deep in the corners of the divertor, is extremely challenging for edge plasma mean-field modelling tools. To circumvent this technical limitation, a geometrical approximation has been proposed, consisting in considering an artificial minor modification of the geometry of the divertor targets plates. In this paper, we investigate how significantly this approximation impacts the output of mean-field simulations. Using the SOLEDGE2D-EIRENE mean-field code which has the unique capability to be able to cope with both the real and the modified geometry, we have performed a density scan in H-mode for pulses in which the outer strike-point lies in the corner of the divertor. We report here how simulations in the artificial geometry differ from the ones in real geometry. At the exception of low density cases, mid-plane profiles in the closed field lines region and the near scrape-off layer are little impacted. Further out however, in flux-surfaces that are concerned by the geometrical modification, we find that modifying the geometry leads to a strong overestimate of the plasma density. The density perturbation is not local and concerns the whole flux surfaces. Although the divertor geometry is modified only on the outer side, the largest impact is found at the inner divertor where densities are systematically overestimated by a factor that can exceed 10 in low density cases in the far SOL and temperature underestimated by 10 to 20eV in most of the studied density range. The near SOL and strike point peak values are also impacted in the same direction with density changes by a factor of 2. As a consequence, the threshold to detachment of the inner divertor is found lower in the approximate geometry than in the real one. Due to the large flux expansion between the outer and the inner target, the difference in plasma is especially sensitive at the top of the inner divertor baffle, which could have consequence on the evaluation of physical sputtering at that critical location.

Keywords: tokamak, modelling, edge, plasma, fluid, corner

1. Introduction

The development of high performance scenarios in the JET tokamak with the metallic ITER-like wall has demonstrated a strong impact of the divertor configuration on plasma performances [1, 2]. Running the plasma with the strike-points located in the corners of the divertor, i.e. as close as possible to the pumping plenums, leads to H98 confinement factors up to 30% larger compared with similar plasmas run with the strike-points located on the vertical plates. Although a few ideas have been put forward to explain such impact (see for example [6]), this behaviour is not fully understood yet.

2D edge mean field codes are key tools in grasping underlying mechanisms. However, the modelling of corner configurations in realistic divertor geometry is challenging, if not impossible, with most edge mean field codes. This is due to the incompatibility between the discretization methods used in these codes and the considered geometry in which divertor tiles intercept flux surfaces in the very near Scrape-Off Layer (SOL). Indeed, the vast majority

of mean-field fluid edge plasma codes uses a flux-surface aligned structured grid in order to improve numerical precision at lower cost in terms of resolution [4, 5, 6]. This is made necessary by the extreme anistropy of the modelled physics between the poloidal direction, which contains the projection of parallel terms, and the direction normal to flux surfaces, along which transport is strongly constrained by the confining magnetic field and is characterized by much slower dynamics. Due to this design choice, most codes are able to model the SOL plasma up to the first tangency point between a flux surface and the first wall. Beyond this point, the gap with the first wall is not covered by the grid and is either considered as vacuum or filled with extrapolated plasma densities and temperatures to provide a background plasma for the neutrals solver. This is not believed to be a major issue when this flux surface is located more than a few SOL e-folding lengths away from the separatrix as the physics of interest occurs entirely within the domain (to the exception of fluxes to the first wall which can be relevant for some specific issues). In some specific configurations however, the clearance between the wall and the separatrix is relatively short compared with typical decay lengths observed in JET, especially at high densities when the SOL density profile strongly broadens [7]. This is especially the case in JET corner configurations where the bottoms of the vertical targets exhibit an apex protruding into the near SOL above the strike-points (see section 2 for an illustration of the geometry).

In order to make the modelling of these cases possible with standard mean-field modelling tools, a possible way to circumvent this limitation was suggested. The idea consists in using a minor artificial modification of the geometry of the divertor tiles surrounding the strike-points, consisting in cutting the bottom tiles of the divertor (tile 3 on the high-field side, tile 7 on the low-field side) along a flux surface sufficiently far from the separatrix (Fig. 1). This way, the simulation domain can extend far enough in the SOL to account for most of the plasma-divertor interaction, assuming that such work-around does not impact significantly the equilibrium of the SOL. The latter assumption needs to be checked in order to assess the exact impact of this geometrical modification and gain confidence on the capability of edge modelling codes to model JET corner configurations.

In this paper, we use the SOLEDGE2D-EIRENE code package to investigate this issue. To do so, we capitalize on the capability of SOLEDGE2D to model the plasma up to the first wall in any magnetic or wall configuration. Specifically, the code is able to model the JET edge plasma both with the real divertor/wall geometry or the modified slanted tile geometry. Based on a JET baseline scenario H-mode pulse in vertical-corner divertor configuration, we have performed a density scan in order to evaluate the impact of the modified geometry on density regimes. The paper is structured as follows: the simulations set-up is described in section 2; key results concerning upstream and divertor conditions are reported in section 3; we then conclude concerning the validity of the possibility to chamfer vertical divertor tiles in the vicinity of the corner to model JET corner configurations in edge mean-field codes.

2. Modelling set-up

The edge plasma of JET is modelled using the SOLEDGE2D-EIRENE 2D mean-field fluid code package [4, 8]. SOLEDGE2D solves multi-fluid equations using the Zhdanov closure [9] which allows the modelling of non trace impurities. In single species simulations such as the ones presented in this paper, the Zhdanov closure reduces to the Braginskii collisional closure [10]. The main specificity of the SOLEDGE2D code in the landscape of mean-field edge plasma solvers is its capability to model the plasma up to the first wall in any magnetic or wall configuration. This feature derives from the technical implementation of Bohm boundary conditions based on the use of penalization methods [11, 13, 12].

JET pulse #90177 at $t = 44.57s$ is used as the reference for the magnetic configuration. It is a low triangularity H-mode plasma with the inner strike point located at the top of tile 3 in the middle of the vertical target and the outer strike point located on the outermost part of tile 6, i.e. in the lower outer corner of the divertor. Figure 1 illustrates the magnetic geometry as well as the mesh and the 2 wall geometries used for this study. The magnetic geometry and the quadrangles mesh of the plasma solver are strictly identical. They differ solely through the shape of the divertor wall in the vicinity of the outer corner of the divertor. In practice, this difference is imposed via local changes in the mask function determining the quadrangular mesh cells that are in the wall and in the triangle mesh used by EIRENE
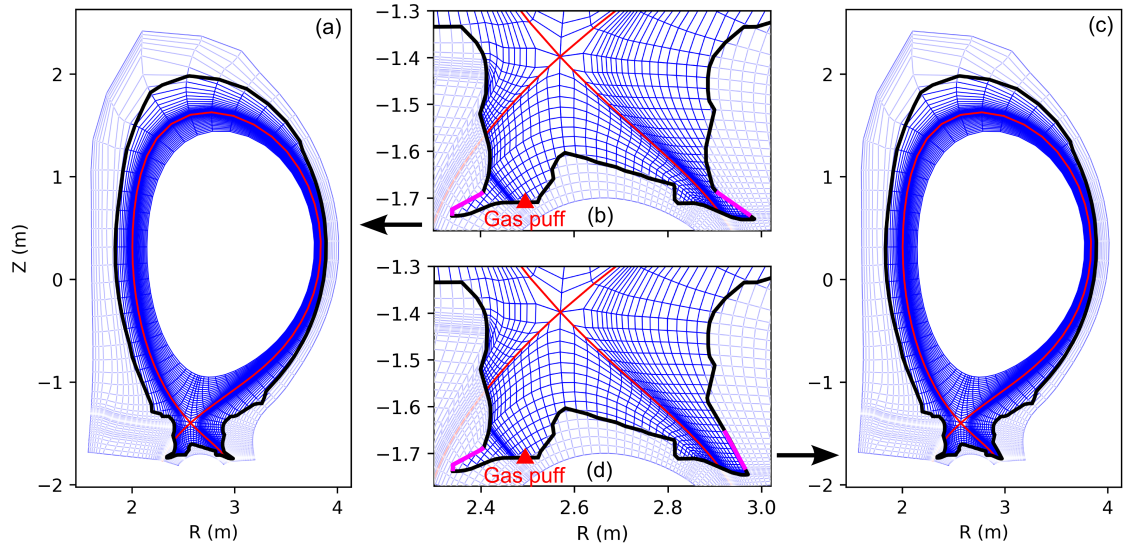
Figure 1: Geometries and meshes used for the set of simulations compared in this paper. (a) and (b): real geometry, respectively whole domain and zoom on the divertor; (c) and (d): slanted tile 7 geometry, respectively whole domain and zoom on the divertor. The red full line is the main separatrix. The red triangles give the location of the gas puff. The parts of the wall highlighted in magenta correspond to the pumps.

for kinetic neutrals. Figure 1 (a) and (b) especially highlight the difficulty associated with modelling such configuration in most edge plasma modelling tools. In the specific case studied here, the clearance between the apex of tile 7 and the separatrix is equal to $1cm$ once remapped in the mid-plane, i.e. slightly smaller than the density decay length. The artificially modified geometry with tile 7 slanted (Figure 1 (c) and (d)) opens this gap up to $2.6cm$.

A pure Deuterium plasma is considered. Perpendicular transport coefficients are given H-mode like profiles inspired from previous studies in JET (Fig. 2). Since the purpose of this study is not to analyse a specific discharge but rather to evaluate the general impact of the artificial modification of the divertor tile's geometry, the exact profile of these coefficients is not central to this paper. It is nevertheless worth pointing out that a similar density scan was run with L-mode like transport coefficients (uniform without barrier) and that the main conclusions of this paper remain valid also in these conditions.

The simulation is driven by an input power of $9.2MW$ entering the simulation domain uniformly through the innermost modelled flux surface and equally distributed on ions and electrons. The plasma is fuelled by a Deuterium gas puff located in the middle of tile 4, i.e. in the private flux region on
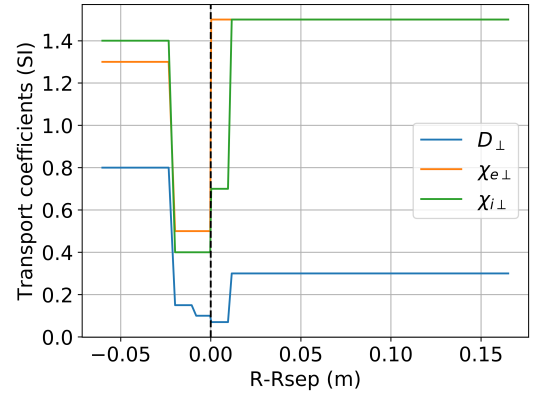

Figure 2: Radial profiles of perpendicular transport coefficients used for this study.

3

the HFS of the horizontal part of the divertor (see Fig. 1). A feedback scheme was used to automatically tune the gas puff so as to match target densities at the separatrix in the outboard mid-plane. The density n_e^u was scanned from $1.5e19m^{-3}$ to $5.0e19m^{-3}$ by step of $0.25e19m^{-3}$, representing a total of 15 simulations for each geometry described above. The wall is considered as being composed of tungsten and characterized by a recycling coefficient $R = 1$ except at the pumping surfaces where $R = 0.95$. The other parameters of the simulation were the following: electron sheath heat transmission factor $\gamma_e = 4.5$, ion sheat heat transmission factor $\gamma_i = 2.5$, flux limiter coefficients for electrons and ions respectively $\alpha_e^{FL} = 0.2$, $\alpha_i^{FL} = 2$.

3. Impact of corner geometry on plasma equilibrium and divertor conditions

We first compare upstream profiles. Fig. 3 shows outboard mid-plane profiles of the density and the electron temperature for all the studied cases. With the exception of the 2 lowest density levels at which the density in the real geometry is up to 20% larger than in the modified geometry, profiles inside the separatrix are insensitive to the geometry of tile 7. In the SOL on the contrary, the real geometry cases are systematically less dense than the equivalent one in the slanted geometry with 2 qualitative trends depending on the density and the distance to the separatrix. For $n_e^u \leq 3.e19m^-3$, real geometry cases are under-dense throughout the SOL. Upstream density profiles even exhibit a non monotonic behaviour in the slanted cases with the presence of a bump at $R - R_{\rm sep} = 1cm$, i.e. the flux surface corresponding to the apex of tile 7. In the real geometry, such non monotonic behaviour does not occur even though a flattening is visible in the first cm of the SOL at low densities. This leads to extremely large differences in the density, by up to a factor of 3 at $R - R_{\rm sep} = 1cm$ at the lowest density. As the upstream density increases, density profiles in the near SOL progressively converge towards each other and end up overlapping in the first cm for $n_e^u > 3.e19m^-3$. Further out, real geometry exhibit a steeper decay length leading to significantly lower densities in the far SOL, with a difference of the order of 30% at $R - R_{\rm sep} = 2.5cm$.

Concerning temperature profiles, differences are less spectacular and can be explained essentially by the behaviour of the density. In the near SOL, real
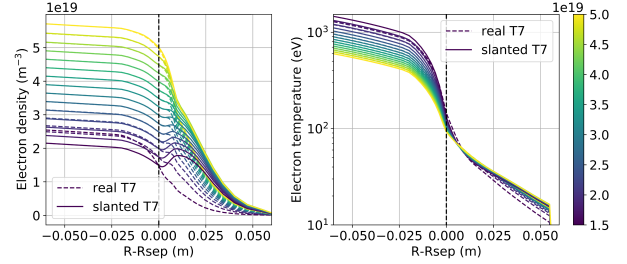

Figure 3: Outer mid-plane profiles of density (left) and electron temperature (right) for all the simulated cases. The color scale corresponds to the various separatrix densities. Dashed lines are for the real tile 7 geometry while full lines are for the slanted tile 7 geometry.

geometry cases tends to be hotter than corresponding slanted tile 7 cases due to the lower density. In the far SOL however, the situation reverses for $R - R_{\rm sep} > 2cm$ with the real geometry cases being systematically cooler.

The 2D distribution of the electron density in the divertor (Fig. 4) is in line with the trends observed in the mid-plane. The lowest density cases exhibit a much larger density everywhere in the main SOL, the difference largely exceeding a factor of 3 in the far SOL. When the upstream density increases, the difference progressively becomes more moderate and localized. In most of the far SOL, the ratio between the 2 cases, is of the order of 2.5 at $n_e^u = 3.25e19m^{-3}$ and 1.75 at $n_e^u = 3.25e19m^{-3}$. Nevertheless, the ratio peaks and remains larger than 3 throughout our density scan in the outer divertor for flux surfaces located between the apex of tile 7 in the real geometry and tile 7 in the slanted case (corresponding to $R - R_{\rm sep} = 1$ to $2.5cm$ in the mid-plane). The difference is also significantly larger along the target plates above the inner strike point, especially on the baffle. We can also note a non-monotonic behaviour in the private flux region, whose density is a factor of 2 larger in the medium density with the slanted tile geometry but is lower at low density and relatively unperturbed at high density.

Similarly to mid-plane profiles, effects on the temperature (not shown here) are milder and can be largely explained by the differences on the density. Flux surfaces corresponding to the region in which tile 7 protrudes in the real geometry ($R - R_{\rm sep} = 1$ to $2.5cm$) are typically 25 to 50% cooler in the vicinity of the outer target in the slanted case. The strongest difference is found at
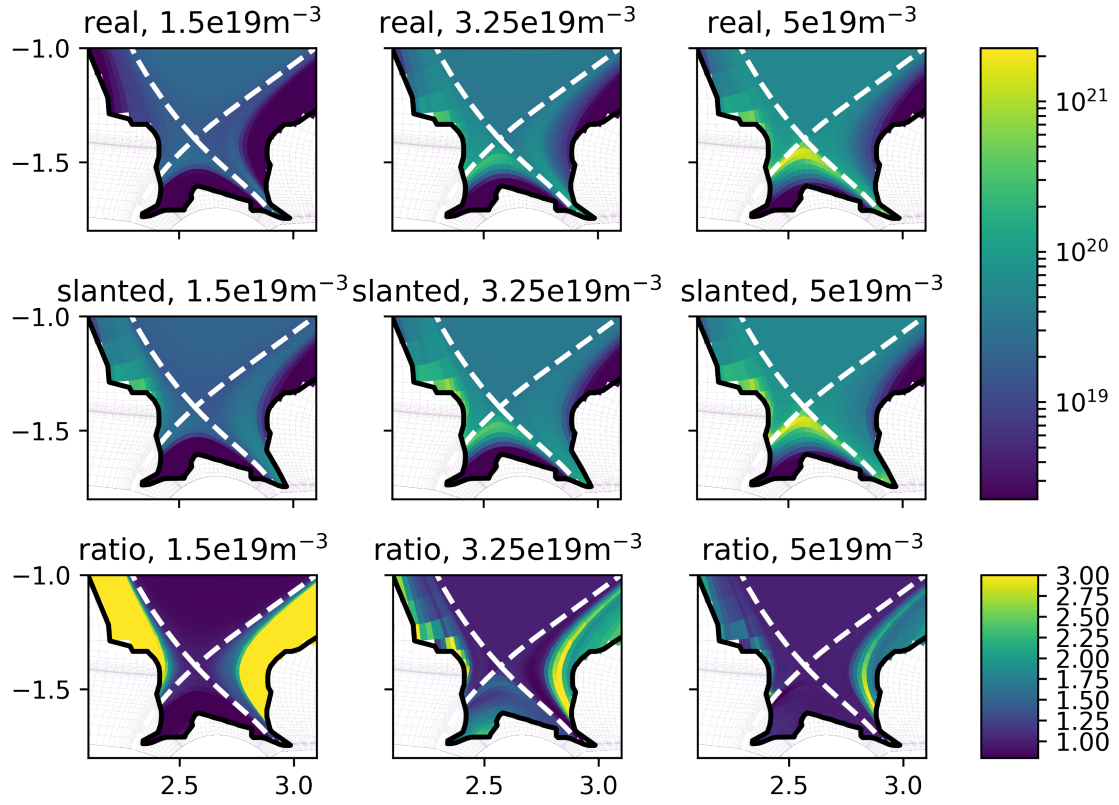
Figure 4: Comparison of the electron density in the divertor in the 2 geometries for 3 density levels. From top to bottom: 1-electron density in m^{-3} in real geometry cases; 2- electron density in m^{-3} in slanted tile 7 cases; 3- ratio of slanted case over real case. From left to right: $n_e^u = 1.5e19m^{-3}$, $3.25e19m^{-3}$, $5.e19m^{-3}$.

the inner target where Te drops by a factor ranging between 2 at $n_e^u = 5e19m^{-3}$ and more than 4 at $n_e^u = 1.5e19m^{-3}$. The latter cooling is especially sensitive at the top of the inner baffle on overdense flux surfaces.

The consequences of these changes on the plasma conditions at the strike-points are shown in Fig. 5. In the vicinity of the outer strike point, if one excludes the part of the wall which is modified and hence cannot be compared, plasma conditions are not changed dramatically. The highest density cases are detached and exhibit identical profiles. For other cases, although the density and temperature can locally change by up to 50% due to minor shifts in the profiles, their shapes as well as their amplitudes follow identical trends. The only significant change is a drop of the ion temperature (not plotted here) in the far SOL at the top of tile 7: in the slanted case the ion temperature at that position is equal to 20eV and barely depends on the upstream density, while in the real geometry it is strongly dependent on n_e^u, ranging from 80eV for $n_e^u = 1.5e19m^{-3}$ down to 30eV for $n_e^u = 5.e19m^{-3}$. This could result on an impact on estimates of sputtering physical in that region.

The situation is different on the inner side where strong trends are found. Let us first notice that the inner strike-point is characterized by much wider target profiles due to the large flux expansion. Significant densities and temperatures are found all the way up to the horizontal surface of the baffle, in agreement with the previous 2D plots. The target density is systematically much larger in the slanted geometry cases than in their real geometry counterparts. 2 regions can be distinguished. Away from the separatrix, for $s_w < 1.94m$ (s_w being the coordinate along the wall) corresponding to $R - R_{\rm sep} > 6mm$, the difference between the 2 cases has a monotonical negative dependency on the upstream density. The difference peaks at $s_w = 1.85m$ corresponding to $R - R_{\rm sep} = 1cm$, i.e. precisely the apex of tile 7 in the real geometry. At that position, the slanted geometry case is overdense by 85% for $n_e^u = 5.e19m^{-3}$ and the difference progressively increases to more than 1000% for $n_e^u = 1.5e19m^{-3}$. Closer to the separatrix, for $s_w > 1.94m$ corresponding to $R - R_{\rm sep} < 6mm$ in terms of magnetic connection to the mid-plane, the impact of the change of geometry is not as striking (although still in the range 100% to 300%) and the monotonical trend with the upstream density is lost, the difference being maximum for interme-
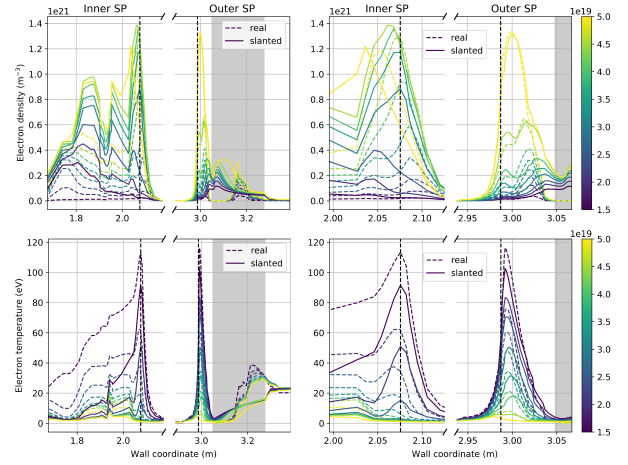

Figure 5: Density and electron temperature profiles along the wall at both strike points. Top: electron density; bottom: electron temperature; left: wide view; right: zoom around strike points. The vertical dashed lines show the location of the separatrix. The greyed areas correspond to the part of the profiles that cannot be directly compared due to a locally different wall shape and in which the wall coordinate was artificially changed to span the same range between cases. Dashed lines are for the real geometry case, full lines for the slanted tile 7 case. The colormap stands for the upstream density at the separatrix n_e^u in m^{-3}. For more clarity only 1/4 of the cases are plotted.

diate values. These changes on the density lead to opposite trends for the electron as well as for the ion temperatures which globally drop in the slanted geometry compared to equivalent real geometry cases. In the near SOL ($s_w > 1.94m$, $R - R_{\rm sep} < 6mm$), the non monotonical behaviour visible on the density is observed also on the temperatures, with a difference ranging between -50 and -75%. Further out, the temperature is the most impacted at lowest densities (-80% from 55eV down to 10eV for T_e, -88% from 90eV down to 10eV for T_i) and the difference progressively reduces when moving up in density (-55% from 7eV down to 3eV for both T_e and T_i at $n_e^u = 5.e19m^{-3}$).

All these trends are summarized in Fig. 6 which shows the evolution of the density, electron temperature T_e, ion temperature T_i and particle flux at the inner and outer strike-points as well as further out in the SOL as a function of the upstream density. The plots highlight again the fact that the geometrical approximation mainly target values at the inner divertor. On the outer side, peak values at the strike point follow extremely similar curves, the only noticeable exception being the electron and ion temperatures in the slanted geometry (and hence

the particle flux at a more moderate level) which exceed those of the real geometry by up to 30% in the range $n_e^u = 2 - 3e19m^{-3}$. In the far SOL, T_e and T_i are systematically lower in the slanted geometry by at least a factor of 2, but the density is larger leading to larger particle fluxes throughout the density scan.

On the inner side, differences are much more pronounced and not only visible in the far SOL. At the strike point as well as in the far SOL, the density is typically at least a factor of 2 larger in the slanted geometry at the exception of the highest upstream densities when the plasma is deeply detached. As a consequence, temperatures are systematically lower. Here again, the temperature does not compensate for the density excess and the particle flux is found larger throughout the scan in the modified geometry. As mentioned earlier, highest density points correspond to detached plasmas at the strike point and roll-over in the particle flux is observed. The slanted tile 7 geometry exhibits a lower upstream density threshold to access detachment with a shift of the order of $0.5e19m^{-3}$ for the maximum of the particle flux. Deviation from the high density regime (degree of detachment departing from 1 as defined in [14]) is observed as early as $n_e^u = 3.e19m^{-3}$ in the slanted geometry while first signs of it occur at $n_e^u = 3.75e19m^{-3}$ in the real geometry.

4. Conclusion

Using the geometrical capability of the SOLEDGE2D-EIRENE code to model the plasma up-to-the-wall in arbitrary geometry, we have investigated the impact of a seemingly minor artificial modification of the geometry of the outer divertor which is necessary to make to model those configurations in most 2D mean-field codes. A density scan in a vertical-corner configuration pure deuterium H-mode plasma has been performed both in the approximate geometry, where tile 7 (bottom vertical tile in the outer divertor) is slightly slanted, and in the real geometry. Comparisons between the 2 cases show a significant impact on the density and temperature equilibria, especially in the far SOL beyond the first flux surface concerned by the modification of the divertor geometry. On upstream profiles first, the density beyond the first surface grazing the tip of tile 7 is found twice as large in the approximate geometry as in the real geometry. This is due to the fact that

corresponding flux surfaces are not screened any more from neutrals recycling from the strike-point by the apex of tile 7 and get artificially fuelled by them. This change in the fuelling distribution has little impact on the plasma conditions at the outer strike-point. In the inner divertor however, the observed impact is much stronger with a shift of the whole divertor in terms of density regime: the plasma is overall denser (up to 1000% in some cases), cooler and detaches earlier than in the real geometry. The effect is especially sensitive in the far SOL for flux surfaces connected to the modified part of tile 7's geometry, but is also important at the strike-point itself where the density changes by typically a factor of 2, and in the very far SOL on the top of the inner baffle, which might have consequences on the evaluation of physical sputtering. The spreading of the perturbation from the far SOL only on the low field side to the whole SOL on the high field side can most probably be explained by the redistribution of density (and momentum/energy sinks) permitted by the neutrals although further studies would be necessary to pinpoint the exact mechanism at play. As a consequence of these changes on plasma conditions, detachment is found to occur earlier in the approximate geometry than in the real one.

Overall, our results demonstrate that care must be taken when dealing with the modelling of corner cases. The minor artificial modification of the divertor geometry suggested to be used to allow the modelling of these cases is not without consequence on the edge plasma equilibrium, even far away from the location of the change. In the cases studied here, we show that the impact on the inner divertor conditions render the use of the approximate geometry impossible to study physics happening in the vicinity of the inner targets. At the outer strike-point and in the upstream near SOL, the impact is relatively low except at low densities. However, we cannot warranty that this later result remains valid in all plasma conditions.
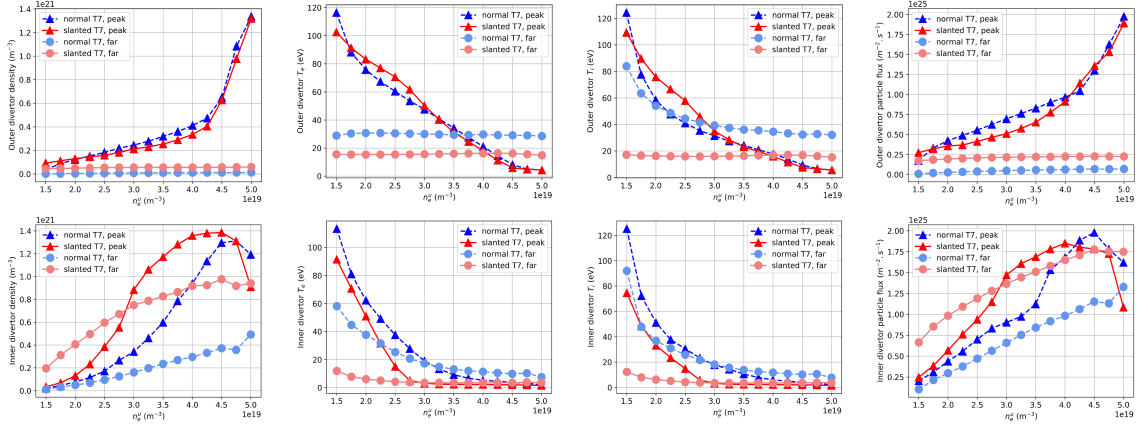
5. Acknowledgements

Figure 6: Electron density, electron temperature, ion temperature and particle flux as a function of the upstream density n_e^u. Top row: outer divertor; bottom row: inner divertor. Dashed lines are for the real geometry cases, full lines for the slanted tile 7 cases. Two values are plotted each time: peak value at the strike point ($s_w \in [2.05, 2.1]\,m$ on the inner side, $s_w \in [2.95, 3.05]\,m$ on the outer side) and a far SOL value at $s_w = 1.85m$ on the inner side ($R - R_{\text{sep}} = 1cm$) and $s_w = 3.28m$ on the outer side ($R - R_{\text{sep}} = 2.7cm$, ie first point of the wall in the far SOL in common between the 2 geometries).

References

[1] P. Tamain et al. J. Nucl. Mater. 463, 450 (2015).

[2] E. Joffrin et al., Nucl. Fusion 57, 086025 (2017).

[3] A. Chankin et al., Plasma Phys. Control. Fusion 61, 075010 (2019).

[4] H. Bufferand et al., Nucl. Fusion 55, 053025 (2015).

[5] S. Wiesen et al., J. Nucl. Mater. 463, 480-484 (2015).

[6] A.V. Chankin et al., Plasma Phys. Control. Fusion 61, 075010 (2019).

[7] A. Wynn et al., Nucl. Fusion 58, 056001 (2018).).

[8] R. Mao et al., Nucl. Fusion 59, 106019 (2019).

[9] V.M. Zhdanov, Transport Processes in Multicomponent Plasma, CRC Press (2002).

[10] S.I. Braginskii, Reviews of Plasma Physics 1, 205-311 (1965).

[11] L. Isoardi et al., J. Comp. Phys. 229, 2220 (2010).

[12] H. Bufferand et al., J. Nucl. Mat. 415, 589 (2011).

[13] A. Paredes et al., J. Nucl. Mat. 438, 625 (2013).

[14] A. Loarte et al., Nucl. Fusion 38, 331 (1998).